Tribology International 165 (2022) 107281

Contents lists available at ScienceDirect

Tribology International

journal homepage: www.elsevier.com/locate/triboint

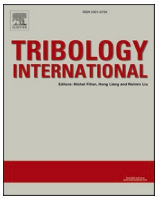

# The tribological behavior of analog mudrock interfaces in dry, water-immersed and guar-gum solution states

J. Ren [a], F. Wang [b], H. He [c], K. Senetakis [a,*]

[a] City University of Hong Kong, Hong Kong, China
[b] Stanford University, USA
[c] Southeast University, Nanjing, China

ARTICLE INFO

*Keywords:*
friction
mudrock
wetting-drying cycle
guar gum

ABSTRACT

The behavior of analog mudrock interfaces was examined at the micrometer scale under various confinements and shear rates in room-dry, water-immersed and guar-gum solution states. The data indicated that the presence of water at the interfaces resulted in a continuous reduction of the friction in comparison to the dry state due to a predominant effect of abrasion, whereas no clear influence on the friction was observed in the shearing cycles involving guar-gum solution. The addition of guar-gum solution had a more notable softening effect which was presented by a larger percentage of reduction in the initial tangential stiffness.

## 1. Introduction

The tribological and mechanical behavior of clays and mudrocks is of major interest in the petroleum engineering research, as the study of the frictional properties of clays/shales and their interactions with proppants comprise a fundamental, though very challenging step in the characterization/stimulation of tight/unconventional reservoirs and the analysis of the hydraulic fracturing process [1–16]. In specific, the studies by Sone and Zoback [1,2] in conjunction with the state-of-the-art review by Zoback and Kohli [11] and the recent findings through microindentation experiments by Kasyap and Senetakis [16], have shown that the structural characteristics of shales/mudrocks govern their anisotropic behavior. However, a large number of factors such as depth, geological and tectonic history, as well as rock composition and the type of experiment that is used to assess the properties of the rock/rock interface, influence the characterization and interpretations from geophysical and geomechanical analyses. Many of these works have highlighted that the tribological study of clay interfaces (or clay-proppant and proppant-proppant interactions) is important to be examined at the level of micrometer-size displacements and that the interaction of proppant-mudrock or proppant-fluid-mudrock interfaces is significantly influenced by the intrinsic properties of the clay. Bandara et al. [7–9] and Ahamed et al. [17] studied the crushing behavior of proppants and their interactions with analog rock subjected to high pressure highlighting the influence of proppant type on the embedment mechanisms. These studies, along with recent works by [3–6,13,14], have developed experimental and analytical approaches which examine the problem of proppant-rock interactions at the small-scale, which is a fundamental step in the analysis of larger-scale systems. Thus, apart from the important insights which are obtained from the study of proppant-proppant interfaces [8,17,18], tribological studies examining the intrinsic behavior of reconstituted clays are particularly useful for a fundamental understanding of the interactions of proppant-fluid-rock systems. For example, the recent literature has suggested that proppant morphology, mudrock type, loading history and condition of the interfaces (e.g., dry or in the presence of fluids of various viscosities), influence the frictional properties of proppant-rock systems [4–6,13,14], which are inherently influenced by both intrinsic properties of the proppant and the rock. However, the examination of mudrock interfaces providing fundamental insights into the way the loading history and surface condition affect their intrinsic behavior is a highly unresearched topic, which should be examined, fundamentally, by constructing reconstituted samples to decouple diagenetic influences and bonding from that of the intrinsic properties of the material.

Examination of mudrock-type interfaces is also of interest in geological engineering and geoscience applications, for example in the study of soft marine deposits [19–21] and the study of structural discontinuities, such as fissures (characterized as cracking or splitting), which are ubiquitous in the natural systems [22–24]. One of the fundamental steps in the analysis of structural discontinuities is the

* Corresponding author.
*E-mail address:* ksenetak@cityu.edu.hk (K. Senetakis).

https://doi.org/10.1016/j.triboint.2021.107281
Received 24 February 2021; Received in revised form 20 August 2021; Accepted 13 September 2021
Available online 20 September 2021

investigation of their frictional response, however previous works have majorly examined the behavior of those systems, predominantly, at larger sliding displacements, which can provide useful information at the steady-state regime, but not complete understanding of the constitutive behavior of interfaces. This would necessitate studies which can quantify tangential (or sliding) stiffness which normally requires very small displacements to be obtained, of the order of a few microns. Additionally, the formation of structural discontinuities results in "scaly-clays" involving different geological processes and ground-environment interactions including tectonic movements, bulk shearing, submarine gravity sliding and unequal expansion during erosion and weathering cycles. The wide range of the scales of the fissures which have dimensions from millimeters to centimeters necessitates the implementation of more comprehensive studies on clays at various sizes, not limited necessarily at the centimeter scale, which is the typical scale used in laboratory tests. Based on these discussions, it is highlighted that the study of the behavior of clay/mudrock interfaces is of interest in a broad range of science and engineering applications encountering various scales and involving the stability of geo-systems, ground-environment interaction problems as well as the study of sedimentary soils/rocks in the presence of fractures [11,12,24].

In the literature, the macro-scale behavior of cohesive geological materials, which include clays and mudrocks, is often interpreted based on continuum mechanics approaches, however several researchers have attempted to treat cohesive soils (clays and some silts) as 'micro-systems', formed by a group (or clusters) of clayey particles. In this way, cohesive soils are analogous to granular materials and the mechanical behavior of the clay microsystem is observed to have a resemblance to that obtained from conventional macro-scale tests. For example, Chang et al. [25] and Yin et al. [26,27] developed a microstructural stress-strain model based on the assumption of treating clay clusters with a mean size of 4 nm as 'grains' and the numerical results predicted by the model matched reasonably well with the experimental results at the macroscopic level. Quantifying the tribological behavior of natural materials in "in-situ" or "reconstituted" state within a scale of micrometers of displacements, is therefore essential in the advancement of contact mechanics models which can be utilized in micromechanical-based (discrete) simulations. Discrete-based simulations use, as input, the force-displacement governing laws and the interface frictional properties of the contacted materials (grain or equivalent grain type) and in recent years, a significant amount of research has been directed in the application of discrete-based numerical analyses into hydraulic fracturing problems which involve the simulation of mudrock-type rocks and proppant-fluid-rock interactions [28–31]. However, the setting of DEM models often ignores real experimental data, which would necessitate complete force-displacement constitutive relationships to be implemented. This gives a lot of scope in the analysis of analog mudrock interfaces at the level of micrometer of sliding displacements. Thus, an experimental investigation into the interface behavior of clay-based materials in the context of force-displacement behavior and interface coefficient of friction would provide, apart from fundamental insights into the tribological behavior of earth materials and ground-environment interaction problems, basic properties which can enhance micromechanical-based analyses in relation to mudrock-type materials and petroleum engineering applications, which was one of the motivations behind this work.

In the present study, an investigation of the shearing behavior of reconstituted kaolinite samples is attempted by means of micromechanical experiments using a custom-built apparatus which accommodates miniature-size specimens. Due to the working principle of the apparatus as well as the much smaller dimensions of the remolded samples in comparison to those prepared in conventional tests, these miniature tests can contribute to investigate the shearing behavior of geological materials at the level of micron displacements. The findings of the previous studies showed that the mechanical properties of clay slopes in the field or clay samples tested through conventional laboratory tests were largely affected by the wetting-drying cycles which are in correspondence with the change of micro-climate conditions and soil-environment interactions [32–38]. However, these works, even though have emphasized on the influence of clay-environment interaction (e.g., wetting-drying cycles) on their frictional behavior and strength, have not discussed comprehensively on their complete constitutive behavior, which necessitates appropriate experimental setups which can quantify sliding stiffness at the level of micron displacements. Therefore, the shear response of the micro-scale kaolinite samples in this study is evaluated by considering various interface conditions including dry state, water-immersed (or water-wetted) state as well as guar gum solution (GG)-wetted state, examining both interface friction, as a fundamental property in tribological studies and the sliding stiffness – displacement relationship, which is important to be obtained for complete constitutive modeling. The application of water and guar gum solution aims at covering fluids of different viscosities. This is particularly useful not only in the study of natural systems, but also in the fundamental understanding of mudrock behavior in hydraulic fracturing applications [4,6].

## 2. Experimental apparatus

The force-displacement relationship and frictional behavior of the miniature kaolinite blocks were investigated using a custom-built micromechanical loading apparatus constructed in the Geomechanics Laboratory of City University of Hong Kong [14,39]. A schematic illustration of the experimental setup is given in Fig. 1. This apparatus is capable in testing the behavior of small-sized specimens (a few millimeters to tens of millimeters in diameter), including natural sand grains, artificial materials or reconstituted soil samples, with various shapes ranging from grain-grain, grain-block to block-block types of contacts. The application of the different combinations of either force or displacement is achieved by two loading arms included in the apparatus; one is oriented in the vertical direction and the other is placed in the horizontal direction. In terms of the vertical loading system, the sliding of an angle bracket connected with a load cell (with a precision of 0.01 N) and an upper sample mount at the tail end is driven by a high-precision servo-motor with a built-in linear stage. For the horizontal loading system, a linear micro-stepping motor with a micro-step size of 0.048 μm is used to control the delicate movements of the loading system. The actuator is settled on an elongated aluminum panel with adjustable feet in order to ensure the level of the horizontal system. Connection components including linear guides (linear bearings), metal sleeves and other mechanical parts are applied to connect the motor with another high-capacity load cell and a sled which is equipped to hold the lower mount well and lower sample mount. The sled is placed on a highly polished aluminum plate with three stainless steel ball bearings in between to minimize the friction generated by the system. The shearing test, which has a similar concept of a direct shear test, is achieved by moving the lower sample through the horizontally placed stepper motor (applying shearing in this way), while the upper sample remains stationary in the horizontal direction with a designated normal load maintained constant at the contact by the vertical system. Two digital microscope cameras are used to adjust the positions of the upper and lower samples and monitor the experimental process. An image of the clay samples in contact taken by the cameras is presented in Fig. 1 as an illustration. The same figure provides a general illustration of the test system (block-block) used in the present experiments.

## 3. Material and sample preparation

Kaolinite, a white to cream-colored clay originated, predominantly, from the weathering of feldspars, is a common type of clay mineral in nature [40]. It has a relatively more stable chemical composition and lower shrink-swell capacity compared to other typical types of clay

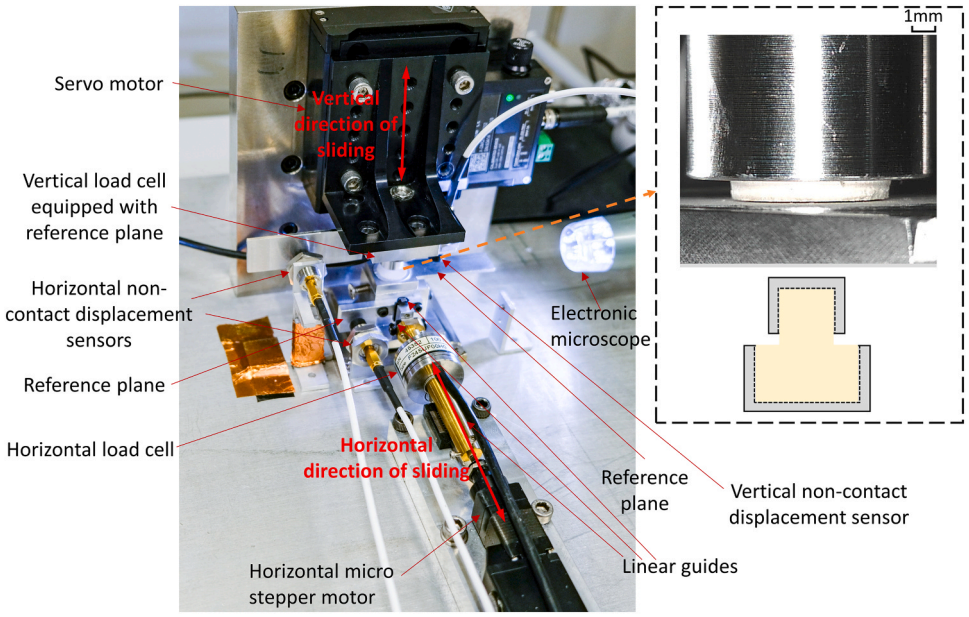


**Fig. 1.** Micromechanical testing apparatus with an inset showing the kaolinite samples in contact.

minerals, such as montmorillonite and illite. The relatively stable characteristics of kaolinite indicate that its volume will not experience a significant change when absorbing or losing water.

The dry kaolinite powder used in this study was commercially available and according to the Atterberg limit tests, the plastic limit and liquid limit of the purchased kaolinite were found to be 29% and 67%, respectively, so that the clay has a plasticity index of 38%. The micromechanical-based tests were designed to be performed on compacted miniature dry kaolinite specimens which were prepared following the key stages illustrated in Fig. 2. Firstly, distilled water was gradually added into the kaolinite powder and during this process the mixture was stirred continuously in order to achieve uniformity. The moisture content was controlled to fall between the plastic limit and liquid limit so that the mixture was at the plastic state which was workable for the subsequent preparation steps. The final water content of the resultant mixture was calculated to be 58%. Afterwards, the moist kaolinite mixture was placed into an oedometer cell (diameter of oedometer ring = 75 mm) and compressed at a maximum pressure of 4.4 MPa to obtain a compacted kaolinite sample. The unloading process was performed once the consolidation was completed at the maximum vertical stress, so that the final sample was overconsolidated. Note that the cell was filled with water during both the loading and unloading

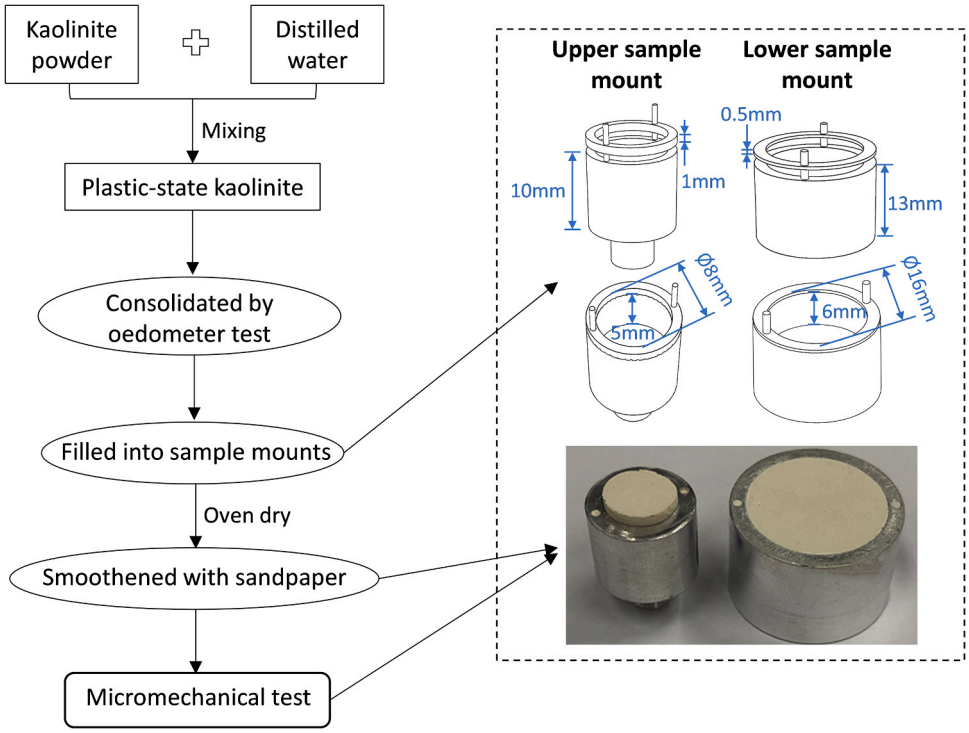


**Fig. 2.** Typical stages of kaolinite sample preparation process with an illustration of the configuration of upper and lower sample miniature mounts designed for the micromechanical tests.

stages (i.e., the specimen was fully immersed in the water bath). The void ratio of the overconsolidated specimen after being removed from the oedometer cell was calculated to be approximately equal to 1.01.

The upper and lower specimen mounts were specially designed for the block over block type of contact and the sketch of the mounts as well as their key dimensions are illustrated in Fig. 2. Both the upper and lower mounts were hollow, which were manufactured to hold the ductile overconsolidated kaolinite under a moist state. Detachable circular rings were placed on the top edge of the sample holders and two slender rods were used to fix them by passing through the holes in both the rings and the surfaces of the sample holders. The thickness of the circular ring on the upper mount was 1 mm while that of the ring on the lower mount was smaller with a value of 0.5 mm. Small volumes of kaolinite were compressed into the mounts with the height slightly above the top plane of the rings so that there was some redundant volume in case that shrinkage takes place during the drying process. The samples were oven-dried at 104 °C for 24 h. The last step of the sample preparation process was to use 600Cw sandpaper to smoothen the uneven dehydrated kaolinite surfaces. For the lower samples, the circular ring was detached from the sample holder before the smoothening process and the layer of the kaolinite sample which was above the top of the mount was removed by the sandpaper. Differently, the circular ring remained on the upper sample mount during the entire smoothening process until the surface of the kaolinite sample was level with the top of the ring. Representative images of the upper and lower kaolinite specimens prepared for the micromechanical-based tests are given in Fig. 2. The top of the upper kaolinite sample was slightly higher compared to the metal surface of the sample mount so that the contact between the surface of the upper mount and the lower kaolinite specimen can be avoided during shearing. Also, based on the dimensions of the sample holders, the top surface area of the lower kaolinite specimen was found to be four times greater than that of the upper kaolinite sample, which guaranteed that there was enough sliding path for the shearing tests to be carried out. The microfabric of the kaolinite sample was evaluated by

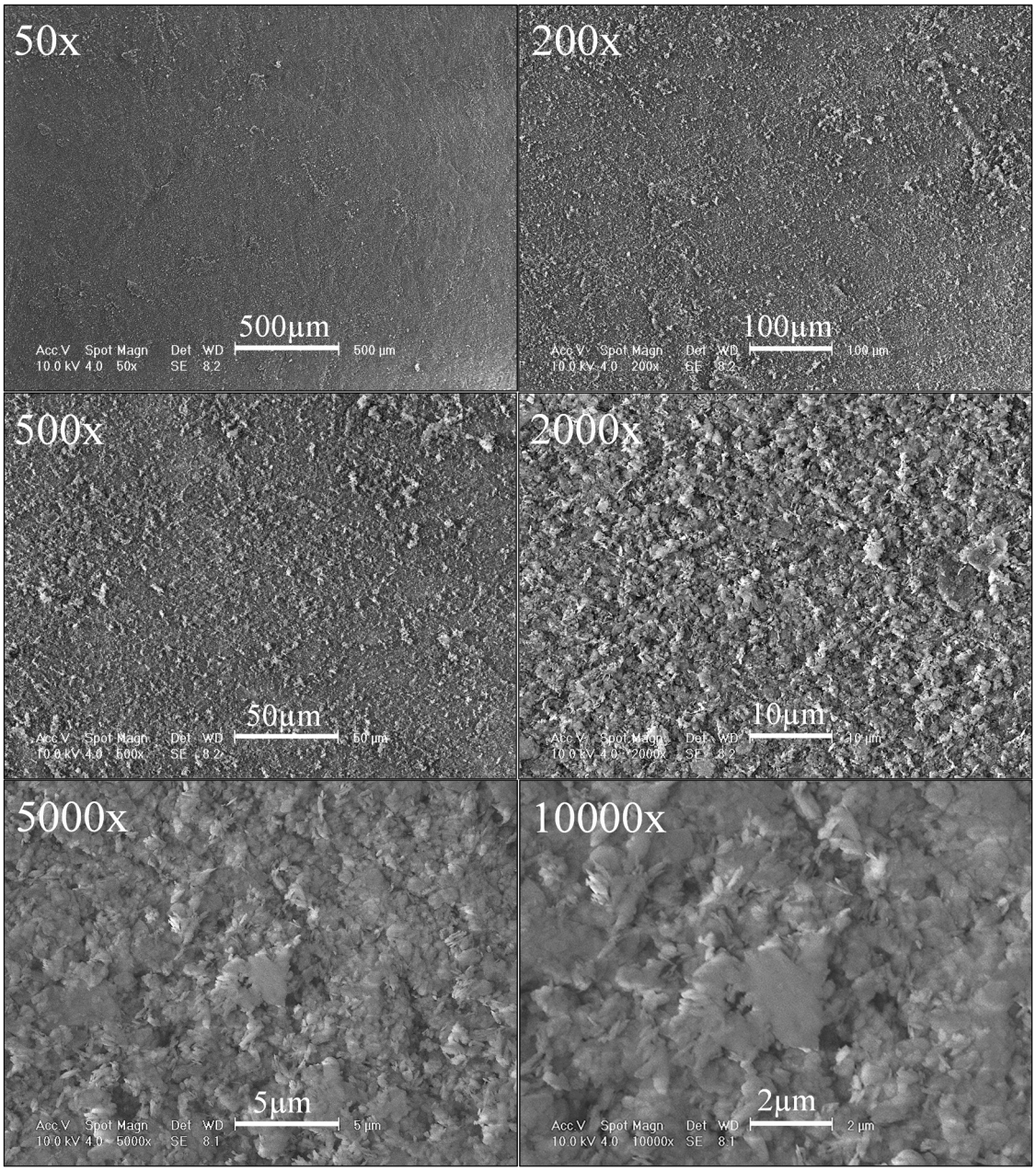


**Fig. 3.** Scanning electron microscope (SEM) images of surfaces of kaolinite samples at different magnifications.

an environmental scanning electron microscope (SEM) (Philips XL30) before the implementation of the shearing tests. The final surface of the kaolinite sample was in general smooth and flat with some shallow scratches created during the sample preparation process and at high magnifications, the aggregation of the clay particles in some areas of the specimen are observed as the scanning electron microscope (SEM) images of Fig. 3 show. Energy dispersive spectroscopy (EDS) analysis was used for the compositional characterization and the respective results from representative samples are given in Fig. 4. Based on this analysis, it was found that Si and Al elements are in similar proportion in the clay, which is expected for a kaolinite-based material [41]. The consistency of the surfaces of the prepared clay specimens was further assessed based on interferometry analyses, in which case the RMS roughness ($S_q$) was measured. A representative image taken from the interferometer and also a summary of the results in terms of RMS roughness are given in Fig. 5. Despite the fluctuations in the data, the $S_q$ values ranged from around 0.665 to 1.27 μm and the coefficient of variation was found to be equal to 17%, which, compared with respective values reported in the literature for various material types [42–44] highlights the highly repeatable surfaces of the blocks based on the sample preparation method adopted in the study.

## 4. Testing program

A total of 23 pairs of kaolinite samples were prepared and subjected to monotonic repeating shearing tests under various testing conditions (details are given in Supplementary Table S1). The pair code used for each specimen was determined based on the surface condition of the sample, the pair number as well as the magnitude of the normal load. The tribological behavior of the clay specimens was investigated by considering four types of surface states: room-dry condition, surfaces wetted by two types of fluids including water and guar gum solution as well as surfaces redried after being wetted by water. The room-dry conditions, provide a quantification of the "intrinsic" tribological behavior of the clay samples. The term "intrinsic", based on geomechanics definition, implies the interface properties of the material decoupling influences of structure (bonding and fabric), or other features which would result from geological processes [45]. Thus, reconstituted specimens are necessary to be constructed and examined for this purpose. Wetting and drying of the surfaces attempted to simulate environmental influences, for example infiltration or evaporation [32–38], while the study of the interfaces in the presence of viscous fluids would be particularly useful in hydraulic fracturing simulation [4,6].

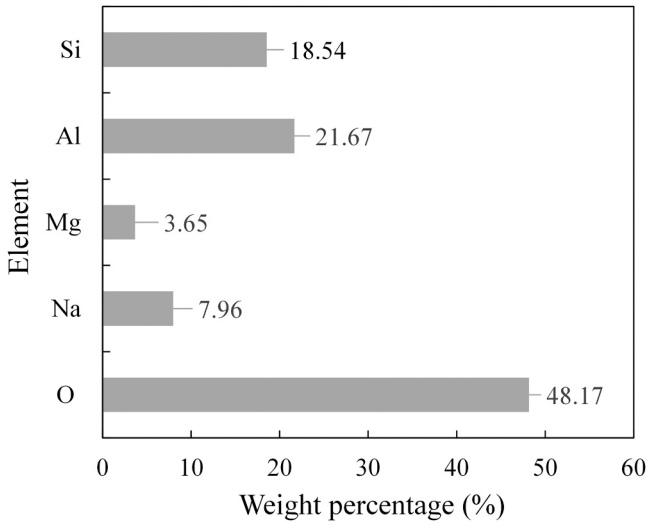


**Fig. 4.** The element weight percentage of the kaolinite samples from energy dispersive spectroscopy (EDS) tests.

In terms of the kaolinite specimen surfaces solely under room-dry condition (termed as "KD"), nine pairs of samples were tested under four different normal loads, namely 1 N, 2 N, 3 N and 5 N applying three to eight shearing cycles to investigate the influences of normal confinement and abrasion. As the apparent contact area of the pair of the specimens was equal to the area of the upper kaolinite sample, the applied normal stress ranged from 20kPa to 100kPa. A range of shearing rates (0.1-631.4 mm/h) was also taken into account to study the potential effect of shearing velocity on the frictional behavior of the dry interfaces, as previous studies have shown some influence of the velocity on the tribological behavior of simulant geological structures in the presence of clay-type gouges [46].

The water (lower viscosity fluid) involved shearing tests, symbolized as "KW", were performed on nine pairs of kaolinite blocks. In this set of tests, the specimens were first sheared under room-dry conditions for four to five cycles and the corresponding results were used as a benchmark for the subsequent tests in different surface conditions. Afterwards, a little amount of distilled water (around 0.5milliliter) was sprayed on the surface of the lower specimen and the subsequent four to six shearing cycles were conducted on the wet interfaces. The dry and wet shearing cycles were expressed by "KW-D" and "KW-W", respectively. For pair codes KW02-1 and KW04-1, the frictional behavior after the contact area redried was further examined by performing one more shearing cycle (termed as "KW-R"). The whole specimens were sheared under three normal confinements (1 N, 3 N and 5 N) and a constant shear rate of 8.8 mm/h. Based on this testing procedure, the tribological behavior of the clay interfaces was examined in dry, wet and re-dried states, thus the frictional properties would result from the coupled influence of wetting-drying and abrasion. One additional test ("KR") was carried out with two shearing cycles to examine the change of the frictional behavior of the clay interfaces under initially dry state and redried state after wetted by water but without shearing the specimens while the surfaces being water-wetted, thus investigating with these tests solely the effect of water absorption (or, alternatively, the influence of wetting-drying cycle) by omitting the possible influence of abrasion. This would provide an understanding of the relative weighted influences of the wetting-drying process and abrasion.

Guar gum solution (a type of biopolymer) with 0.6 wt% concentration was used as a fluid of higher viscosity to investigate the tribological behavior of the kaolinite blocks and compare the results with those of the dry specimens and interfaces in the presence of water (samples with guar gum solution were coded as "KG"). Guar-gum, as a biopolymer-based viscous fluid, has also been investigated in other studies in relation to analog proppant-rock systems [4,6]. Since the viscosity of the guar gum fluid changes with time after its preparation, at least two hours were allowed for the stabilization of the viscosity before the solution was used for the shearing tests [47]. The viscosity of the 0.6 wt% guar gum solution after 12 h of preparation was measured to be 1778mPa•s at 24 °C under a shearing rate of about $10^{-3}$ $s^{-1}$. Similar to the water involved tests, three dry shearing cycles were conducted first ("KG-D") and then the consecutive cycles were performed in the presence of the viscous guar gum solution ("KG-G"). As this type of fluid has a shear thinning behavior [48], shearing velocities from 0.6 to 261.5 mm/h were considered to evaluate potential shearing rate effects on the frictional behavior of the samples.

## 5. Results and discussion

### 5.1. Comparison of the coefficient of friction between dry and wet interfaces

Representative results from the miniature shearing tests of kaolinite specimens in terms of shear load against shear displacement under both dry and wet interface conditions are given in Fig. 6. The applied normal load was 1 N and the experimental data of the first five dry shearing

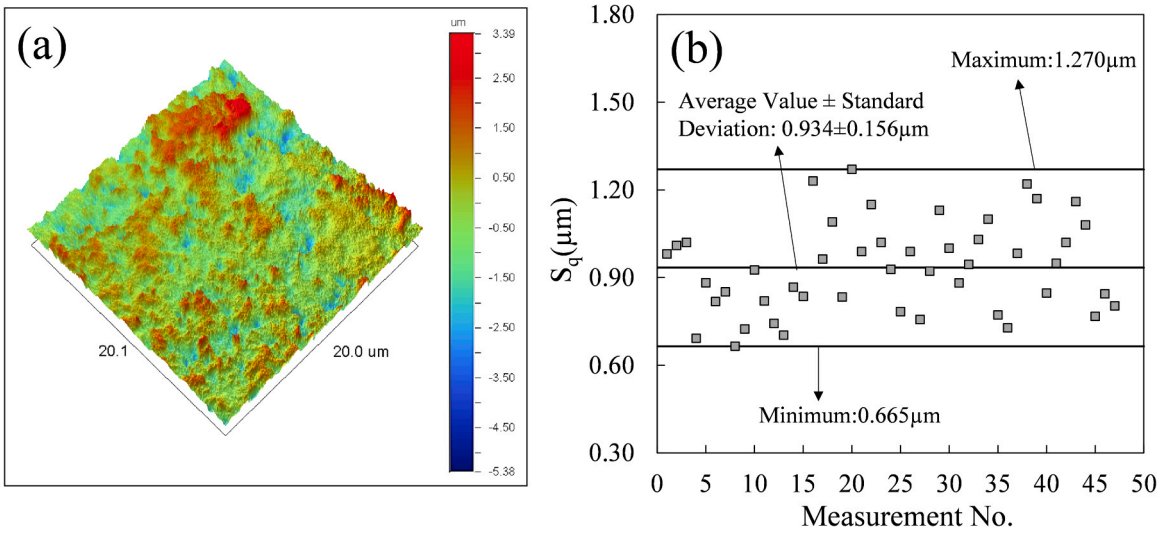


**Fig. 5.** Surface roughness of the kaolinite samples measured by an optical surface profiler (a) a representative surface profile (b) summary of the roughness values.

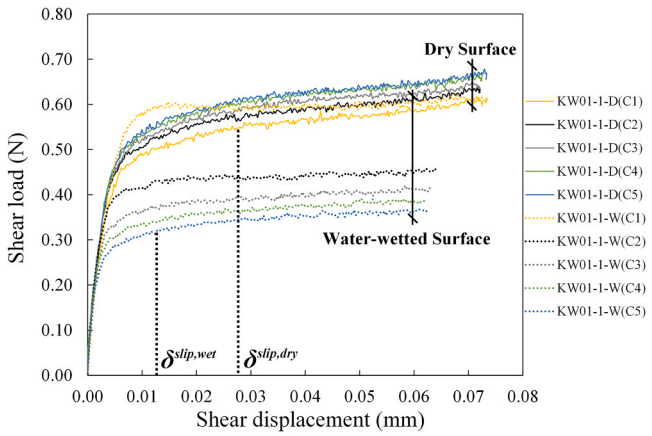


**Fig. 6.** Representative shearing load against displacement curves of dry and wet (water) cycles of pair KW01–1.

cycles are indicated by solid lines, while dotted lines correspond to the successive cycles of the surface wetted by water. These curves are distinguished in two regimes of behavior. In the first regime, the shear load at the contact increased nonlinearly with increasing shear displacement showing a trend of gradual reduction of tangential stiffness, as a result of the elastic-plastic induced deformations during shearing. In the second regime, the curves reached a plateau indicating microslip or steady-state stage sliding, which was achieved when the shear load equaled to the product of the interface coefficient of friction (denoted as μ) and the normal load ($F_N$). A threshold displacement, termed as slip (or microslip) displacement, $\delta^{slip}$ (after [49]), was used to separate the two regimes and the corresponding slip displacements for dry cycle 1 and wet cycle 5 are marked in Fig. 6 as an indication. In terms of the second regime of dry interfaces, the frictional response of the specimens was characterized by microslip rather than steady state sliding. A similar observation was reported in the micromechanical tests by Kasyap and Senetakis [41] on coated quartz grains with clayey microparticles. This is contributed by the continuous micro breakdown of asperities which has been reported for both natural and engineered materials [42,50,51]. Particularly for the relatively soft interfaces of kaolinite blocks, this condition applies even at low normal loads, but for grain-to-grain contacts of quartz particles, this may be a more dominant mechanism at higher normal loads. For the given specimen (Fig. 6), the increase of shearing cycles led to a very slight increase of the interface friction from 0.58 to 0.64 for the dry condition, which suggests a minor contribution of abrasion influences if the surfaces are sheared in a nominally dry state. Opposite to the dry interfaces, the wetting process (adding water at the interface) resulted in a steady-state behavior at larger displacements rather than microslip. Another important contribution of the wetting of the surfaces was that in the presence of water, the repetition of shearing cycles had a dominant role in reducing the coefficient of friction to values of the order of 0.35 (indicating a reduction of 45% compared with the interface friction of the dry samples). The major reduction of the coefficient of friction took place after the completion of the first two wet shearing cycles, indicating a significant contribution of the coupled influence of wetting process and abrasion in the reduction of the frictional resistance at the interfaces of the kaolinite specimens.

It is worth noting that the first wet cycle showed very different characteristics in comparison to the dry shearing cycles, on that (i) the frictional resistance decreased after wetting, (ii) the curves for the wet samples exhibited a peak, and this peak depended on the magnitude of the applied normal load and (iii) abrasion was more dominant compared with that on dry samples. In Fig. 7, representative curves of the relationship between the shear load and shear displacement under 1 N, 3 N and 5 N of normal loads are plotted, which include the last dry shearing cycle, the first and the second wet shearing cycles. The shear load of the virgin wet cycle firstly ascended to its peak after the initial non-linear regime and beyond which, the shear strength experienced a continuous decrease reaching, approximately, a steady state. Because of the presence of the thin water film in the wetted samples, the peak shear strength is speculated to be the result of cohesion or van de Waals forces (acting as attractive forces), which vanished rapidly after a short shearing path took place, as demonstrated by the post-peak reduction of the shear load. The percentage difference between the peak and steady-state shear strengths decreased at lower normal loads (in specific from 19% at 5 N to 5% at 1 N of normal load for the example in Fig. 7). Data from element-size specimens published in the literature also suggest that for overconsolidated cohesive soils, the shear stress - displacement curves derived from direct shear or ring shear tests have a peak which is followed by a reduction of the frictional resistance, indicating a cohesive mechanism contributing to the shear strength of clayey samples. At larger displacements, the steady-state shearing resistance corresponds to the residual strength, in which condition clay particles have been oriented parallel to the direction of shearing [52]. A similar phenomenon was observed in shearing tests on yellow clay-steel composite interfaces performed by Kocserha and Gömze [53], which study reported a strong orientation of the muscovite flakes in the slipping direction after the

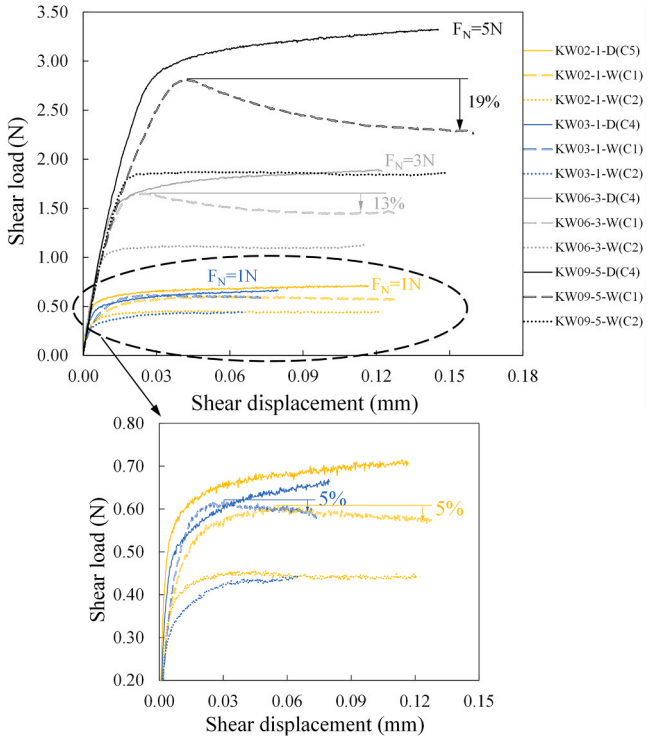


**Fig. 7.** Plots of the last dry, the 1st as well as the 2nd wet (water) shear cycles from representative specimens sheared under three normal loads.

completion of the tests.

The results in terms of the average microslip/steady-state shear loads of the virgin shearing cycles of specimens with dry interfaces and the first to fourth shearing cycles of the water-wetted interfaces are plotted against the normal load in Fig. 8, where the friction envelopes are also plotted showing the resultant slope and coefficient of determination. Based on the trendlines, the interface friction angle (ϕ) of the dry state was found to be about 32° and the value of the first wet shearing cycle decreased to around 26° (note: the slopes were independent on the normal load). In addition, the interface friction declined accordingly as the number of the wet shearing cycles increased as shown in Fig. 8. Okawara et al. [54] carried out shear box tests on clay samples at dry and wet states and the friction angles of the two states were observed to be about 26° and 13°, respectively, on the basis of the residual stress versus vertical stress curves. Direct shear tests under consolidated-drained condition were performed on zeolitic soil (mainly composed of silts and clays) specimens by Yukselen-Aksoy [55] and the internal friction angle was disclosed to be around 35°, similar as that obtained from the dry kaolinite interfaces.

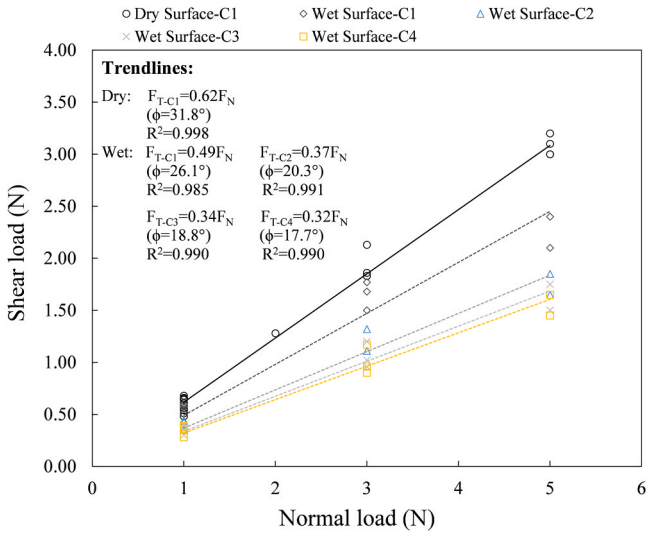


**Fig. 8.** Strength envelopes for dry state kaolinite samples-virgin shearing cycle and wet (water) state kaolinite samples-1st to 4th shearing cycles.

### 5.2. *Influence of wetting-drying cycles and abrasion on the interface friction*

A summary of the total set of tests including dry and wet interfaces (using water as the fluid) are given in Fig. 9. The vertical axis of the plot corresponds to an average value of the coefficient of friction at the steady state (or microslip) regime, while the horizontal axis expresses the successive number of shearing in the whole wetting-drying process.

The dry specimens had μ values which ranged from 0.58 to 0.71 based on the virgin shearing cycle. These values are much higher compared with kaolinite-coated quartz grain interfaces tested by Kasyap and Senetakis [41] (average μ of around 0.25 as reported in that study) and relatively higher compared with decomposed rocks which have developed a clay-type coating on their surfaces because of weathering of feldspars and micas [42,56]. Based on Fig. 9, the interface friction of the kaolinite specimens generally remained stable as the dry shearing cycles increased with some specimens showing slightly increasing trend. Representative SEM photos of the surface conditions of the lower and upper kaolinite specimens before and after five dry shearing cycles (normal confinement equaling to 3 N) are given in Supplementary Fig. S1. It is shown by the SEM images, at two magnifications, that only shallow shearing tracks could be observed (marked with the red boxes), which manifested the limited abrasion effect caused by the dry shearing process. The wetting process of the kaolinite interfaces led to a significant reduction of the friction coefficient and also manifested a major influence of the number of shearing cycles (at the cycle no.8, which corresponded to wet conditions, μ values ranged from around 0.29–0.40). The data suggest a lubrication influence of the water film at the interface which is the coupled result of abrasion (by repeating the shearing following the same paths) and duration of time after the samples were initially wetted. For a few samples, after the last shearing test at wet condition (cycle no.11 in Fig. 9), the specimens were left to dry out at room environment for around 12 h, and subsequently they were subjected to one additional cycle of shearing in an apparent dry state. In this case, an increase of μ was observed as a result of the drying process, but the final values were lower compared with that of the virgin shearing of the dry samples (prior to the wetting process). This suggests that although there is an influence of the time allowed for the water to be

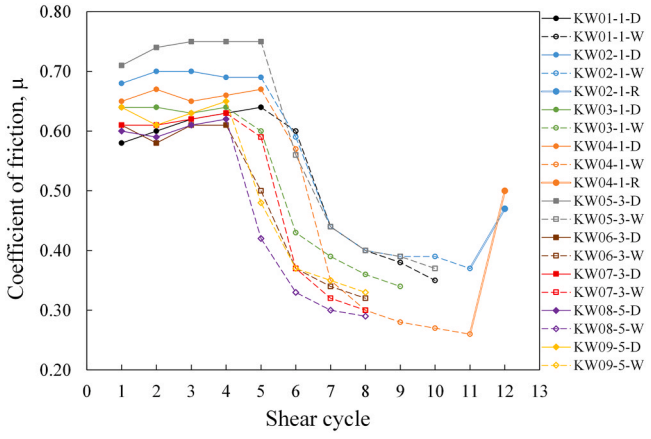


**Fig. 9.** Coefficient of friction against shearing cycles of kaolinite specimens tested under dry and wet (water) states.

absorbed by the clay samples on their interface friction (manifested by the continuous decrease of μ during the tests on wetted specimens), there is also a more dominant influence of abrasion. By comparing the shearing response between the redried interface and the initial dry interface of specimens KW02–1 and KW04–1, the percentage drop of friction coefficient was found to be about 30% and 23%, respectively, as a final result of abrasion. Supplementary Fig. S2 presents the SEM images of the surface conditions of one representative kaolinite sample (lower and upper specimens showed similar phenomenon) after five dry and subsequently five water-wetted shearing cycles performed under 3 N of normal load. Unlike the solely dry shearing cycles, clear shearing tracks, corresponding to the relatively dark areas in the SEM photos, were detected after the wet shearing cycles. At higher magnifications (500× and 800×), clay microparticles in some regions were observed to be flattened/smoothened due to the abrasion effect. For a selected case, a sample (KR01-1) was allowed, after being wetted, to dry out without performing shearing tests (i.e. wetting and drying were not accompanied by shearing tests) and so, dry surfaces were examined before and after wetting excluding the influence of abrasion (Fig. 10). These data indicated that the interface friction was not affected by the wetting-drying process if no shearing takes place, and thus the coupled influence of wetting and abrasion is manifested only when the samples are subjected to repeated shearing in wet condition.

### 5.3. Influence of wetting-drying cycles on the tangential stiffness

Even though the frictional response of interfaces has been examined comprehensively in the literature, the tangential stiffness and stiffness reduction curves have been majorly overlooked within a tribological perspective. In the present work, apart from the parametric study investigating the influence of repeated shearing and surface condition on the coefficient of friction of the analog mudrock interfaces, additional insights were attempted to be obtained with respect to the tangential stiffness. According to the representative shear load-shear displacement curves of pair KW01-1 given in Fig. 6, the tangential stiffness, $K_T$, at a given shear displacement was analyzed by differentiating the shearing load over the shearing displacement and the results are plotted in Fig. 11. The $K_T$ values of the five dry shearing cycles are represented by the filled markers, while those for the water-wetted shearing cycles are illustrated by hollow markers. The results suggest that: (i) within the scatter of the data, the initial tangential stiffness, $K_{T0}$ (defined at the smallest resolvable displacements), decreased for the tests after wetting (ii) for both dry and wet interfaces, the tangential stiffness was significantly influenced by the displacement magnitude, but stiffness decreased faster for the wet samples.

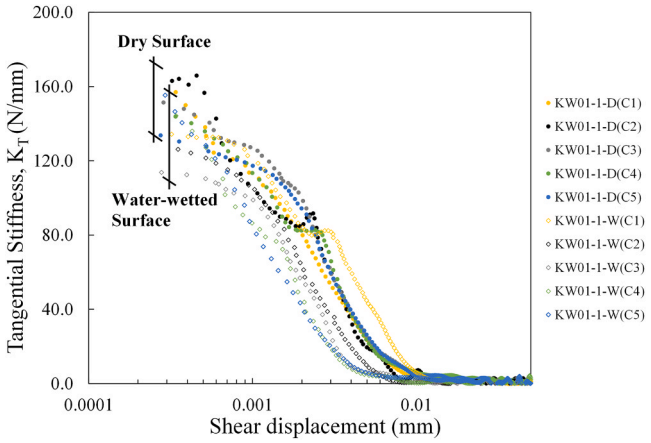


**Fig. 11.** Representative tangential stiffness against shear displacement curves of dry and wet (water) shear cycles of pair KW01-1.

A theoretical curve of the change of the initial tangential stiffness of the kaolinite interfaces during the entire wetting-drying process was drawn based on the general trend observed from the whole set of water involved tests (Fig. 12). The addition of the water considerably reduced the initial tangential stiffness because of the coupled influence of water absorption at the interface and abrasion, which was revealed by the subsequent wetting and redrying cycles (this process, even though results in an increase of $K_{T0}$, the initial stiffness values remained lower in magnitude compared with the virgin "dry" cycles). Different from the continuous decrease of the frictional values due to the repeating shearing process in wet condition, only the first wet shearing cycle had a measurable influence in the decrease of the tangential stiffness and the values remained relatively stable in the consecutive shearing cycles performed on the wet contacts. The corresponding tangential stiffness reduction curves were analyzed based on the shearing response curves of pair KR01-1 given in Fig. 10 and the results further manifested that the sole water absorption of clay samples without abrasion taking place on the wet interface had a negligible impact on the $K_{T0}$ values. In other words, the process of abrasion was a more influential factor leading to the alteration of the stiffness under the wet state.

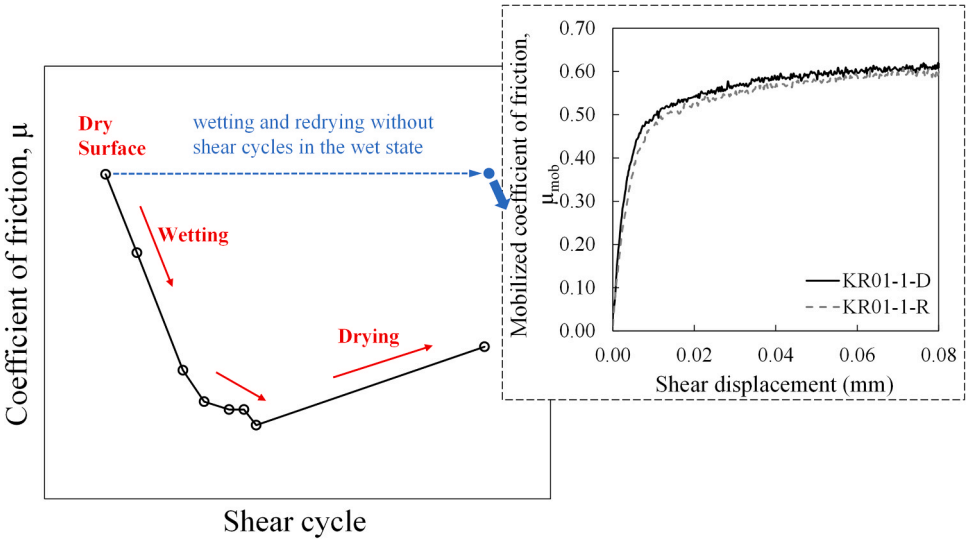


**Fig. 10.** Theoretical trend of the change of coefficient of friction under dry and wet (water) states.

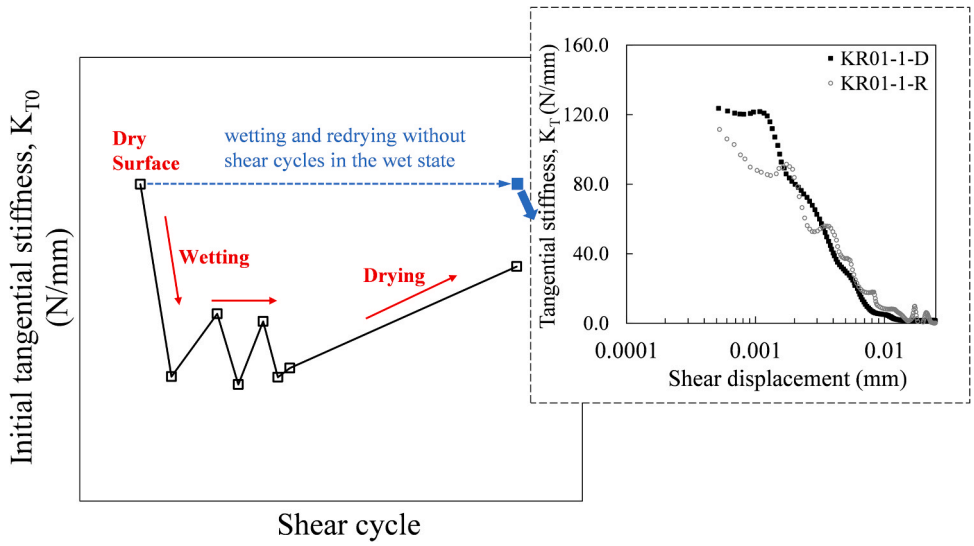


**Fig. 12.** Theoretical trend of the change of initial tangential stiffness of kaolinite specimen interface under dry and wet (water) states.

### 5.4. Analytical model-virgin shear cycle at dry interface

A hyperbolic model, which was originally proposed to express the shear stiffness (modulus) reduction curves of soils in the small to medium strain range (i.e., shear strain $\leq 1\%$) [57], was modified and adopted to depict the tangential stiffness reduction curves of the micro-scale kaolinite specimens under dry shearing (only fitting the virgin cycles). By replacing shear modulus (expressed in Pa) with tangential stiffness (expressed in N/m or N/mm), strains with displacements and using, similar as in the original version of the modified hyperbolic model, two fitting parameters as (i) reference displacement (being reference strain in the original model) and (ii) curvature shape coefficient, the modified hyperbolic model proposed by Darendeli [57] is reformed for the interface shearing tests as:

$$\frac{K_T}{K_{T0}} = \frac{1}{1 + (d/d_{ref})^a} \tag{1}$$

where ($K_T/K_{T0}$) is the normalized tangential stiffness with respect to the initial stiffness, (d) is the shear displacement, while ($d_{ref}$) and (a) are the reference displacement and the curvature shape coefficient, respectively. The reference displacement, which is the shear displacement for $K_T/K_{T0} = 0.5$, and the curvature shape coefficient are two fitting parameters that determine the overall position and linearity of the model curve. Representative examples of the implementation of the modified hyperbolic model on the experimental results of three specimens tested under different magnitudes of normal load are given in Fig. 13(a), where the experimental data are plotted in markers and the fitted curves are illustrated in lines. The values of the best-fitted parameters are marked, and the results showed that within the scatter of the data, the fitting curves matched satisfactorily well with the experimental results. Nonetheless, due to the fluctuation of the experimental data, some parts of the measured data could not be perfectly depicted by the model curves, such as the initial shear regime of tests KW06-3-D(C1) and KW09-5-D(C1). Within the three tests presented in Fig. 13(a), both the reference displacement and the curvature shape coefficient increased as the normal load increased.

Based on the measured $K_{T0}$, the $K_T$ value at any shear displacement can be determined based on Eq.(1). Attempts were made to derive the shear load - shear displacement relationship with the model predicted $K_T$ values, with which the shear load at displacement $d_1$ can be calculated based on the previous shear load at displacement $d_0$ as follows:

$$F_{T,d1} = F_{T,d0} + K_{T,d0}(d_1 - d_0) \tag{2}$$

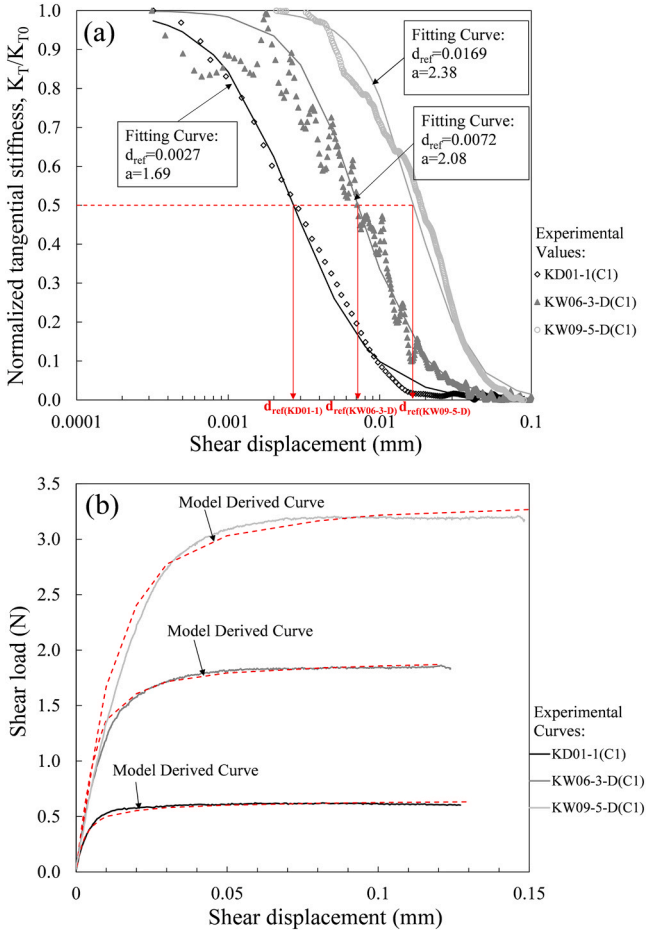


**Fig. 13.** (a) Implementation of the modified hyperbolic model on the experimental normalized tangential stiffness against shear displacement (b) Comparison between model derived curves and experimental curves of shear load versus shear displacement.

When compared with the experimental data, the derived shear load was found to be slightly lower in magnitude than the experimental data, indicating a minor underestimation of the $K_T$ values from the model which could be attributed to two factors: (i) Part of the experimental

stiffness reduction curve could not be perfectly fitted by the model; (ii) The experimental $K_T$ value at a given shear displacement presented in this study was taken as the average slope of a few experimental data points (around 10–20) in order to obtain a relatively smooth curve, which may result in the slightly lower $K_T$ values than the actual instantaneous $K_T$ values. Based on a trial-and-error approach, a constant correction factor of 1.25 was applied to adjust the model fitted $K_T$ values and the predicted results were noticed to have a good agreement with the experimental data of the representative tests, as illustrated in Fig. 13 (b).

According to the best-fitted curves applied for the whole experimental data of the virgin dry shearing cycles, a roughly linear relationship was found between the reference displacement and the normal confinement from Fig. 14(a), despite some scatter in the data at 5 N of normal load. The curvature shape coefficient, which was not systematically affected by the normal load within the range of the normal loads covered in the present study, had an average value and a standard deviation of 1.91 ± 0.24 (Fig. 14(b)). Thus, Eqs. (1)–(2) in conjunction with the model parameters as presented in Fig. 14 provide a preliminary but solid basis to utilize constitutive models stemming from real experimental data in discrete-based computer simulations which attempt to examine "clay microsystem" simulants.

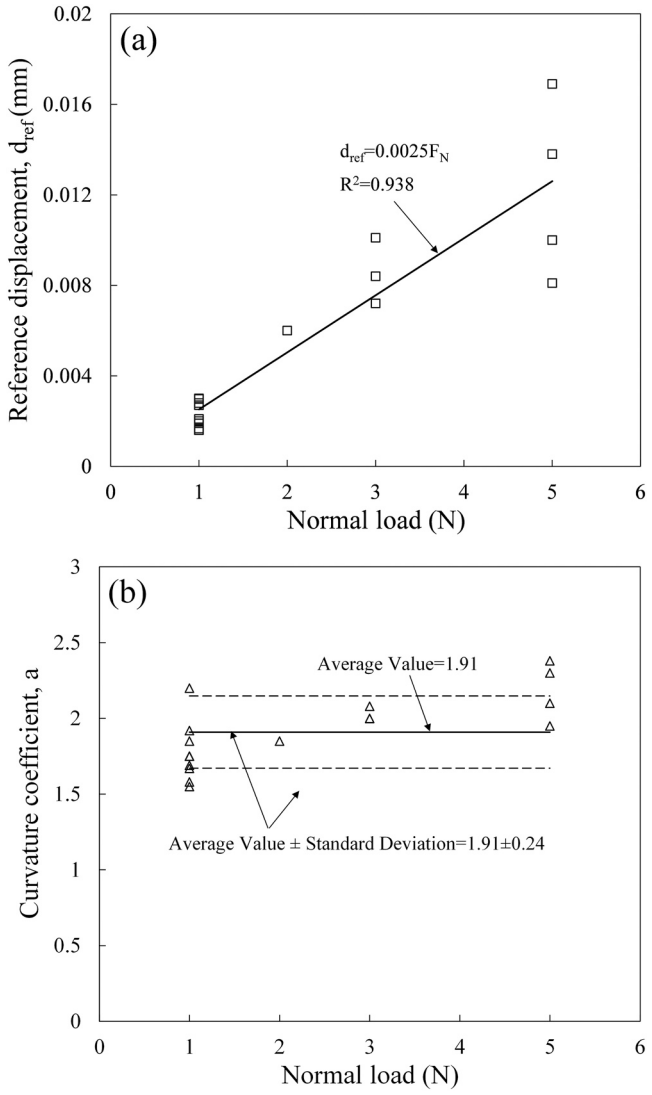


**Fig. 14.** (a) Relationship between the magnitude of normal load and the reference displacement (b) Summary of curvature coefficient against the magnitude of normal load.

### 5.5. Effects of guar gum solution on the shearing response

The effect of 0.6 wt% guar gum solution (GG) on the shearing response of the kaolinite interfaces was investigated performing multiple cycles of repeating shearing on given pairs of specimens under both dry and GG-wetted conditions, adopting the similar concepts with the series of water-wetted tests discussed in Section 5.1. The shear load - shear displacement curves of a few characteristic cycles of shearing on a representative pair of specimens are presented in Fig. 15(a) to illustrate the typical effects of GG wetting on the shearing response of the kaolinite interfaces. By comparing the two consecutive shearing cycles under dry and GG-wetted conditions (i.e., KG02-1-D(C3) and KG02-1-G (C1)), the presence of guar gum solution at the interface noticeably decreased the slope of the shearing response curve in the initial displacement regime while the maximum shear resistance markedly increased in the presence of guar gum at the interface. The increase of the shear strength was only observed in the first cycle with the consecutive cycles having steady-state shear loads that were close to those of the dry shearing cycles.

A summary of the frictional behavior of the whole set of guar gum solution involved tests is given in Supplementary Fig. S3, where the friction coefficients are plotted against the number of the shearing cycles. The results of the initial three dry cycles are presented by filled markers connected by solid lines and those of the successive cycles under GG-wetted condition are illustrated by hollow markers connected by dotted lines. Note that for pairs KG02-1 and KG04-1, the shear load of the first guar gum wetted cycle did not reach a steady state, as shown in the representative curve termed as KG02-1-G(C1) in Fig. 15(a), and

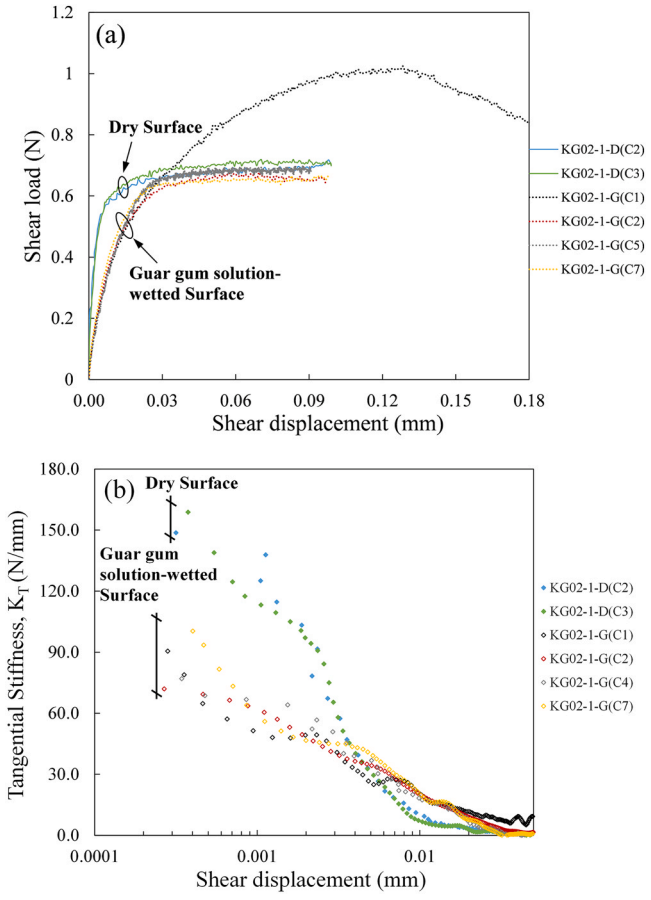


**Fig. 15.** (a) Representative shear load against shear displacement curves of dry and wet/viscous (0.6 wt% guar gum solution) shear cycles of pair KG02-1 (b) Representative tangential stiffness against shear displacement curves of dry and wet/viscous (0.6 wt% guar gum solution) shear cycles of pair KG02-1.

hence, the friction value was roughly estimated by taking the shear strength recorded at the largest shear displacement (i.e., shear load was taken as 0.8 N at a displacement of 0.18 μm for cycle KG02-1-G(C1)). The addition of the guar gum solution to the specimen interface notably increased the coefficient of friction by magnitudes of at least 0.1–0.3 (an increase of about 15–50%) for specimens KG01, KG02 and KG04; however, the μ value slightly dropped after the solution was added for specimen KG03. Apart from the attractive forces developed in the presence of the thin fluid layer, the viscous nature of the guar gum solution is believed to be one of the main reasons for the significant increase of shear strength from shear cycle 3 to cycle 4, which is also time-dependent, reflected by the drop of the frictional values noticed for the specimens of the subsequent shearing cycle (i.e., from shear cycle 4 to cycle 5) resulting from the absorption of fluid by the clay surface. Unlike the frictional behavior of the kaolinite interfaces in water-wetted condition, showing a continuous reduction of shear strength (mainly because of the abrasion), compared with the relatively more complicated boundary condition and rheological properties of the guar gum fluid, there was no consistent influence of guar gum solution observed as the shearing cycles progressed. The abrasion effect under the GG-wetted state was speculated to be coupled with the developed adhesive forces due to the viscosity of the solution that could provide extra shear strength in this scenario. It is important to notice that, as also the study by [39] has shown, the increase of the shearing resistance or lubrication influences (i.e., decrease of friction) when viscous fluids interfere at the contacts of geological materials, would depend to an important extend on the viscosity of the fluid. A fluid which increases the resistance against sliding at the discontinuities of mudrocks could be considered as a mitigating means against micro-seismicity, which is a topic that worth further investigation.

Representative tangential stiffness against shear displacement curves of pair KG02-1 are plotted in Fig. 15(b). From the comparison between the dry and GG-wetted shearing cycles, the addition of the guar gum solution resulted in a reduction of the initial tangential stiffness and an increase of slip displacement. A summary of the relationship between the normalized initial tangential stiffness (the $K_{T0}$ values of the repeating shearing cycles were normalized with respect to the first shearing cycle, $K_{T0,1}$) and the number of shearing cycles is given in Supplementary Fig. S4. The data indicate a reduction in $K_{T0}$ values of the order of 30–70% after guar gum was added, which implies a stronger influence of guar gum solution in the stiffness reduction compared with that of water-wetted interfaces. Despite the minor fluctuations, the initial tangential stiffness remained relatively stable in the successive guar gum solution involved shearing cycles, which suggests limited influence of abrasion after the first cycle. Additionally, Supplementary Figs. S3 and S4 depict the shearing velocity at which the data points were obtained for the interface friction and tangential stiffness. Within the range of shearing velocities from 0.6 mm/h to 261.5 mm/h covered in the study, there was not observed a systematic influence of sliding rate on the interface behavior of the specimens, even though, the literature would suggest that the shearing velocity is one of the main factors that would influence the frictional behavior of the shale rock-silica contacts in the presence of guar gum solution [4].

## 6. Summary and conclusions

The tribological behavior of analog mudrock by means of reconstituted kaolinite block samples was examined using a custom-built micromechanical testing apparatus that adopted the similar concept of the conventional direct shear test but with a focus of performing shearing on miniature specimens with scales down to the micrometer level. The tribological behavior of kaolinite samples under both dry and wet conditions was investigated under a range of normal load magnitudes and shear velocities. In this study, the wet state was achieved by adding distilled water or 0.6 wt% guar gum solution at the interfaces, thus examining fluids of different viscosities. The addition of fluids, either with little viscosity or with relatively higher viscosity, simulates clay fissures subjected to wetting-drying cycles in the field as well as other processes involving soil-environment interactions and it finds applications in the simulation of hydraulic fracturing processes.

The data analysis showed that under dry conditions, the friction of the kaolinite specimens was not affected by the abrasion process within the range of the normal loads covered. By contrast, the presence of water at the interface led to a significant reduction of the coefficient of friction and amplified abrasion influences. The presence of guar gum solution influenced the frictional values compared with the case of dry interfaces, but because of the coupled influence of adhesive force development, abrasion and time, there was not found a clear relationship between coefficient of friction and number of shearing cycles. The presence of water at the kaolinite block interfaces also altered the constitutive behavior of the specimens transforming the frictional response at larger displacements from a microslip-mode to a steady-state sliding mode. However, additional experiments performed decoupling the influences of wetting-drying cycles and abrasion, showed that the interface friction was not affected by the wetting-drying process if no shearing takes place, and thus the coupled influence of wetting and abrasion is manifested only when the samples are subjected to repeated shearing in wet condition. In terms of constitutive behavior (tangential stiffness – displacement relationship), both water and guar gum solution decreased the initial tangential stiffness of the miniature kaolinite interfaces, with the latter (with much higher viscosity) having a more pronounced softening effect. Based on the tangential stiffness degradation curves, the slip displacement was extended by the addition of guar gum solution, while the addition of water showed the opposite trend. The results were further analyzed implementing, after appropriate modifications, a hyperbolic-type model which has been commonly used in the modeling of element-size specimens; this analysis led to the quantification of the model (fitting) parameters of reference displacement and curvature coefficient as a function of normal load. These results can be particularly useful as input in discrete-based simulations of "clay microsystems", which is a promising area of research in tribological and geoscience applications.

## CRediT authorship contribution statement

**J. Ren:** Conceptualization, Methodology, Data curation, Writing of this work. **F. Wang:** Conceptualization, Methodology, Data curation, Writing of this work. **H. He:** Conceptualization, Methodology, Data curation, Writing of this work. **K. Senetakis:** Conceptualization, Methodology, Data curation, Writing of this work..

## Declaration of Competing Interest

The authors declare that they have no known competing financial interests or personal relationships that could have appeared to influence the work reported in this paper.

## Acknowledgements

The work described in this article was fully supported by grants from the Research Grants Council of the Hong Kong Special Administrative Region, China, Project No. "CityU 11210419" and Project No. "CityU 11214218". The authors would like to thank the anonymous reviewers for their constructive comments that helped us to improve the quality of the work.

## Appendix A. Supporting information

Supplementary data associated with this article can be found in the online version at doi:10.1016/j.triboint.2021.107281.

## References


[1] Sone H, Zoback MD. Mechanical properties of shale-gas reservoir rocks – part 1: static and dynamic elastic properties and anisotropy. Geophysics 2013;78(5): D381–92.
[2] Sone H, Zoback MD. Mechanical properties of shale-gas reservoir rocks – part 2: ductile creep, brittle strength, and their relation to the elastic modulus. Geophysics 2013;78(5):D393–402.
[3] Xiao H, Liu S, Wang D. Tribological properties of sliding shale rock-alumina contact in hydraulic fracturing. Tribol Lett 2016;62(20):20. https://doi.org/10.1007/s11249-016-0667-x.
[4] Zhang H, Liu S, Xiao H. Frictional behavior of sliding shale rock-silica contacts under guar gum aqueous solution lubrication in hydraulic fracturing. Tribol Int 2018;120:159–65.
[5] Zhang H, Liu S, Xiao H. Sliding friction of shale rock on dry quartz sand particles. Friction 2019;7(4):307–15.
[6] Zhang H, Liu S, Xiao H. Tribological properties of sliding quartz sand particle and shale rock contact under water and guar gum aqueous solution in hydraulic fracturing. Tribol Int 2019;129:416–26.
[7] Bandara KMAS, Ranjith PG, Rathnaweera TD. Proppant crushing mechanisms under reservoir conditions: insights into long-term integrity of unconventional energy production. Nat Resour Res 2019;28(3):1139–61.
[8] Bandara KMAS, Ranjith PG, Rathnaweera TD, Wanniarachchi WAM, Yang SQ. Crushing and embedment of proppant packs under cyclic loading: an insight to enhanced unconventional oil/gas recovery. Geosci Front 2019. https://doi.org/10.1016/j.gsf.2020.02.017.
[9] Bandara KMAS, Ranjith PG, Rathnaweera TD. Laboratory-scale study on proppant behaviour in unconventional oil and gas reservoir formations. J Nat Gas Sci Eng 2020;78:103329.
[10] Wang J, Ge H, Wang X, Shen Y, Liu T, Zhang Y, et al. Effect of clay and organic matter content on the shear slip properties of shale. J Geophys Res: Solid Earth 2019;124:9505–25.
[11] Zoback MD, Kohli AH. Unconventional reservoir geomechanics: shale gas, tight oil, and induced seismicity. Cambridge University Press; 2019.
[12] Kohli AH, Zoback MD. Frictional properties of shale reservoir rocks. J Geophys Res: Solid Earth 2013;118(9):5109–25.
[13] He H, Senetakis K. A micromechanical study of shale rock-proppant composite interface. J Pet Sci Eng 2020;184:106542.
[14] He H, Luo L, Senetakis K. Effect of normal load and shearing velocity on the interface friction of organic shale–proppant simulant. Tribol Int 2020;144:106119.
[15] Jia Y, Fang Y, Elsworth D, Wu W. Slip velocity dependence of friction-permeability response of shale fractures. Rock Mech Rock Eng 2020;53:2109–21.
[16] Kasyap SS, Senetakis K. Characterization of two types of shale rocks from Guizhou China through micro-indentation, statistical and machine-learning tools. J Pet Sci Eng 2022;208:109304. https://doi.org/10.1016/j.petrol.2021.109304.
[17] Ahamed MAA, Perera MSA, Dong-yin Li, Ranjith PG, Matthai SK. Proppant damage mechanisms in coal seam reservoirs during the hydraulic fracturing process: a review. Fuel 2019;253:615–29.
[18] Yang L, Wang D, Guo Y, Liu S. Tribological behaviors of quartz sand particles for hydraulic fracturing. Tribol Int 2016;102:485–96.
[19] Yin Z-Y, Chang CS, Karstunen M, Hicher P-Y. An anisotropic elastic-viscoplastic model for soft clays. Int J Solids Struct 2010;47(5):665–77.
[20] Yin Z-Y, Karstunen M, Chang CS, Koskinen M, Lojander M. Modeling time-dependent behavior of soft sensitive clay. J Geotech Geoenviron Eng 2011;137 (11):1103–13.
[21] Yin Z-Y, Yin J-H, Huang H-W. Rate-dependent and long-term yield stress and strength of soft Wenzhou marine clay: Experiments and modeling. Mar Georesources Geotechnol 2015;33:79–91.
[22] Vannucchi P, Maltman A, Bettelli G, Clennell B. On the nature of scaly fabric and scaly clay. J Struct Geol 2003;25(5):673–88.
[23] Stark TD, Eid HT. Slope stability analyses in stiff fissured clays. J Geotech Geoenviron Eng 1997;123(4):335–43.
[24] Bjørlykke K. Petroleum geoscience: from sedimentary environments to rock physics. 2nd ed. Springer; 2010.
[25] Chang CS, Hicher P-Y, Yin ZY, Kong LR. Elastoplastic model for clay with microstructural consideration. J Eng Mech 2009;135(9):917–31.
[26] Yin Z-Y, Chang CS, Hicher P-Y, Karstunen M. Micromechanical analysis of kinematic hardening in natural clay. Int J Plast 2009;25:1413–35.
[27] Yin Z-Y, Xu Q, Chang CS. Modeling cyclic behavior of clay by micromechanical approach. J Eng Mech 2013;139(9):1305–9.
[28] Burukhin AA, Kalinin S, Abbott J, Bulova M, Wu YK, Crandall M, et al. Noval interconnected bonded structure enhances proppant flowback control. Soc Pet Eng 2012. https://doi.org/10.2118/151861-MS.
[29] Shimizu H, Murata S, Ishida T. The distinct element analysis for hydraulic fracturing in hard rock considering fluid viscosity and particle size distribution. Int J Rock Mech Min Sci 2011;48:712–27.
[30] Zeng J, Li H, Zhang D. Numerical simulation of proppant transport in hydraulic fracture with the upscaling CFD-DEM method. J Nat Gas Sci Eng 2016;33:264–77. https://doi.org/10.1016/j.jngse.2016.05.030.
[31] Zhang F, Zhu H, Zhou H, Guo J, Huang B. Discrete-element-method/computational-fluid-dynamics coupling simulaiton of proppant embedment and fracture conductivity after hydraulic fracturing. SPE 2017;22(2). https://doi.org/10.2118/185172-PA.
[32] Allam MM, Sridharan A. Effect of wetting and drying on shear strength. J Soil Mech Found Div 1981;107(4):421–38.
[33] Petry TM, Armstrong JC. Stabilization of expansive clay soils. Transp Res Rec 1989; 1219:103–12.
[34] Dif A, Bluemel W. Expansive soils under cyclic drying and wetting. Geotech Test J 1991;14(1):96–102.
[35] Wright SG, Zornberg JG, Aguettant JE. The fully softened shear strength of high plasticity clays. Austin, Texas, USA: Center for Transportation Research, The University of Texas at Austin; 2007.
[36] Kampala A, Horpibulsuk S, Prongmanee N, Chinkulkijniwat A. Influence of wet-dry cycles on compressive strength of calcium carbide residue–fly ash stabilized clay. J Mater Civ Eng 2014;26(4):633–43.
[37] Khan MA, Hossain MS, Khan MS, Samir S, Aramoon A. Impact of wet-dry cycles on the shear strength of high plastic clay based on direct shear testing. In: Geotechnical Frontiers: Geotechnical Materials, Modeling, and Testing. Orlando, Florida: ASCE; 2017. p. 615–22.
[38] Charkley FN, Zhang K, Mei G. Shear strength of compacted clays as affected by mineral content and wet-dry cycles. Adv Civ Eng 2019;2019:1–8.
[39] Ren J, Li S, He H, Senetakis K. The tribological behavior of iron tailing sand grain contacts in dry, water and biopolymer immersed states. Granul Matter 2021;23(1): 12. https://doi.org/10.1007/s10035-020-01068-0.
[40] Grotzinger J, Jordan TH. Understanding earth. 7th ed. Macmillan Learning; 2014.
[41] Kasyap SS, Senetakis K. A micromechanical experimental study of kaolinite-coated sand grains. Tribology Int 2018;126:206–17.
[42] Sandeep CS, Senetakis K. Effect of Young's modulus and surface roughness on the inter-particle friction of granular materials. Materials 2018;11(2):217.
[43] Sandeep CS, Todisco MC, Nardelli V, Senetakis K, Coop MR, Lourenco SDN. A micromechanical experimental study of highly/completely decomposed tuff granules. Acta Geotech 2018;13(6):1355–67.
[44] Sandeep CS, Li S, Senetakis K. Scale and surface morphology effects on the micromechanical contact behavior of granular materials. Tribol Int 2021;159: 106929. https://doi.org/10.1016/j.triboint.2021.106929.
[45] Atkinson J. An introduction to the mechanics of soils and foundations. UK: McGraw-Hill International Series in Civil Engineering; 1993.
[46] Kasyap SS, Senetakis K. An experimental investigation on the tribological behaviour of nominally flat quartz grains with gouge material in dry, partial saturated and submersed conditions. Pure Appl Geophys 2020;177(7):3283–300.
[47] Mudgil D, Barak S, Khatkar BS. Guar gum: processing, properties and food applications—a review. J Food Sci Technol 2014;51(3):409–18.
[48] de Vicente J, Stokes J, Spikes H. Soft lubrication of model hydrocolloids. Food Hydrocoll 2006;20(4):483–91.
[49] Sandeep CS, Senetakis K. An experimental investigation of the microslip displacement of geological materials. Comput Geotech 2019;107:55–67.
[50] Ni J, Zhu Z. Experimental study of tangential micro deflection of interface of machined surfaces. J Manuf Sci Eng 2001;123(2):365–7.
[51] Sandeep CS, Senetakis K. Grain-scale mechanics of quartz sand under normal and tangential loading. Tribol Int 2018;117:261–71.
[52] Okawara M, Mitachi T. Basic research on mechanism of residual strength of clay. In: Di Benedetto H, Doanh T, Geoffroy H, Sauzéat C, editors. Proceedings of the third international symposium on deformation characteristics of geomaterials, 22-24 Sep., Lyon, France. A.A. Balkema Publishers; 2003. p. 505–10.
[53] Kocserha I, Gömze LA. Friction properties of clay compounds. Appl Clay Sci 2010; 48(3):425–30.
[54] Okawara M, Hisatsune T, Mitachi T, Saino T. Microscopic structure and spectroscopic property of the shear surface at the residual state of clay. Clay Sci 2010;14(6):211–8.
[55] Yukselen-Aksoy Y. Characterization of two natural zeolites for geotechnical and geoenvironmental applications. Appl Clay Sci 2010;50(1):130–6.
[56] Sandeep CS, Senetakis K. The tribological behavior of two potential-landslide saprolitic rocks. Pure Appl Geophys 2018;175:4483–99.
[57] Darendeli MB. Development of a new family of normalized modulus reduction and material damping curves (PhD Thesis). The University of Texas at Austin; 2001.